# Development of a Schumann-Resonance Station in Mexico: Preliminary Measurements

*F. P. Sierra[1], H. S. Vázquez[1], M. E. Andrade[2], B. Mendoza[2] and D. Rodríguez-Osorio[2]*

[1]Instituto de Geofísica y Astronomía, AMA-CITMA
La Habana, Cuba

[b]2Instituto de Geofísica
Universidad Nacional Autónoma de México
México D.F., C.P. 04510 Mexico
E-mail: blanca@geofisica.unam.mx

## Abstract

Here, we present preliminary results obtained from a station that monitors the Schumann resonance between ~0 Hz and 50 Hz. The station is currently under development in Mexico (latitude 19° 48' 19" N, longitude 101° 41' 39" W). This station is the first of its kind in the region that includes Mexico, the Caribbean and Central America. The station has two inductive antennas, one for each horizontal magnetic field component. We measured Schumann Resonance harmonics at 7.74, 14.11 and 20.22 Hz. We present the frequency and amplitude behavior of the first three Schumann Resonance harmonics between 00:00 and 08:00 LT along several days during April, 2012.

Key words: Schumann resonance; receiving antennas; active filters, operational amplifiers, electromagnetic measurements.

## 1. Introduction

The phenomenon known as the Schumann resonance (SR) was hypothesized in the 1950s [1]. The space between the Earth's surface and the lower ionosphere forms a capacitor, the Schumann-resonance signals being the electromagnetic resonances of this cavity. These signals are measured in the extremely low frequency (ELF) band of ~0 Hz to 50 Hz. The Schumann-resonance frequencies are given by the following equation:

$$f_n = \frac{c}{2\pi a}\sqrt{n(n+1)},$$

where $f_n$ is the corresponding harmonic, $a$ is the Earth's radius, and $c$ is the speed of light. The fundamental mode is 10.6 Hz, and the first four harmonics are at 18.4 Hz, 26 Hz, 33.5 Hz, and 41.1 Hz. The first definite experimental confirmation of the Schumann resonance was obtained by Balser and Wagner (1960) [2], showing spectral peaks near 7.8 Hz, 14.2 Hz, 19.6 Hz, 25.9 Hz and 32 Hz.

The Schumann-resonance variations are caused by global atmospheric lightning, and geophysical and solar activity. The Schumann resonance presents clear daily and seasonal changes [3-5]. The study of the Schumann resonance has become very important, as these signals can monitor seismic events [6, 7], climate [8-11], the ionosphere [3], solar activity [12-14], or could even impact human health [15, 16].

The design and construction of dipole antennas to detect the electrical component is almost impossible, due to the very long wavelengths associated with the Schumann resonance. For instance, for a frequency of ~8 Hz, the wavelength is 37,500 km. The best option is then to use inductive antennas to detect the magnetic component of the signal [17, 18].

The Schumann resonance's electric and magnetic amplitudes are very low, and can be masked by natural and man-made interference. That is why the antenna's receivers must have special characteristics concerning their internal noise, input impedance, filtering, and voltage gain ($G$) [18].

 ISSN 1045-9243/2012/$26 ©2014 IEEE 

Here, we present the development of a station that monitors the Schumann resonance, located in Coeneo, Michoacán, México (see Figure 1). With geographic latitude 19° 48' 19" N and longitude 101° 41' 39" W, and magnetic coordinates 29° N in latitude and 174° W in longitude, the station is at 1964 m of altitude. It is important to point out that this station is the first of its kind in the region that includes Mexico, the Caribbean and Central America.

## 2. Materials and Methods

We have three basic elements in the Schumann-resonance station's hardware: 1) the antenna, 2) the receiver, and 3) the data-acquisition system.

### 2.1 Antenna

The inductive antenna has the following characteristics: it is 200 cm in length, 5 cm in exterior diameter, and 4 cm in internal diameter. The coils are warped on a high-magnetic-permeability material (permalloy), and encapsulated in an aluminum tube, which in turn is inside a glass-fiber tube. The extremes are sealed with non-ferric materials. The cables exit from one of the coil's ends. The internal structure of the antenna is shown in Figure 2. The antenna's coils are segmented into eight parts: this design responds only to the ease of their manufacture. By having an iron core (permalloy), the antenna does not substantially change its properties as a sensor responsive to the detected signals. The two antennas that measure the two horizontal components of the magnetic field were oriented north-south and east-west, using a compass.

Both the antennas and receptors were located 100 m from the laboratory where the acquisition system is. The antennas were placed 20 cm above the surface level on concrete blocks. The receivers are automatically fed with batteries, charged by a solar panel. All of the system is far from iron elements or structures, as well as from the 60 Hz industrial energy web.

### 2.2 Receiver

The receiver has a simple design, based on the use of instrumental operational amplifiers. We chose an open available design by Hans Michlmayr (http://www.vlf.it/inductor/ulfpreamp_schema.gif). It has eight operational amplifiers. Five of the operational amplifiers suppress the detected local noise in the 50 Hz to 60 Hz band, and a low-pass filter delimits the receiver band between ~0 Hz and 50 Hz. The rest of the operational amplifiers perform as dc amplifiers, giving a dc exit signal with variable components in the 0 Hz to 50 Hz band. This exit signal is adjusted in offset in such a way that it delivers to the acquisition system a signal approximately between ±6 V.

We are interested in registering the two horizontal north-south and east-west signal components. The Schumann-resonance station therefore has two amplifiers. Each amplifier separately processes the mentioned components, delivering them into independent channels of the acquisition system.

## 3. Acquisition System

The analog signals are delivered by a bifilar cable through the amplifiers: they have a dc component with fluctuating


**Figure 1. A map showing the location of the Schumann-resonance station in Mexico (ERS-01) with geographic latitude 19° 48' 19" N and longitude 101° 41' 39" W, and magnetic latitude 29° N and longitude 174° W.**

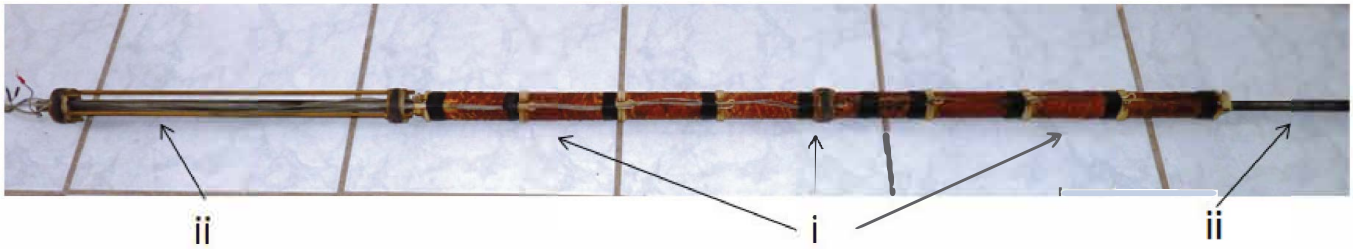


**Figure 2a. The internal structure of the antennas: eight coils connected in series (i); permalloy-steel core, protruding 50 cm from the coils (ii).**

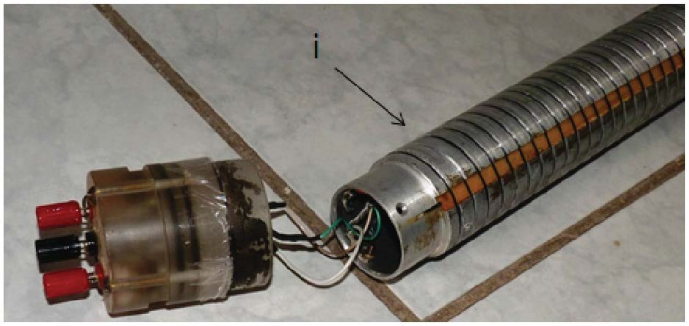


**Figure 2b. The internal structure of the antennas: An aluminum tube (i) as an electrostatic shield.**

**Figure 2c. The internal structure of the antennas: Each coil has about 12000 turns of wire, 0.14 mm in diameter. The exterior diameter of each coil is 31.1 mm.**


**Figure 2d. The internal structure of the antennas: The core diameter (i) is 14.75 mm. The length of each coil is 113.55 mm, and the total number of coils is 1000 mm. The core length is 2000 mm.**

signals detected by the antenna. They are sent to the connectors (SB-68-NI) and, from there, through the 5HC68-EP-NI cable to the 6036E PCI acquisition card. In this card, the signals are converted into digital format to be interpreted by the *LabView* software. The data is sampled every ten minutes and stored in hourly, daily, and monthly files. The spectral plots are generated using the fast Fourier transform (FFT) of the *Microcal Origin* program.

## 3. Development

The antennas are highly hermetic; however, as they are outside, we have to protect them from the natural elements. They are oriented in $x$, $y$, where $x$ coincides with north-south and $y$ coincides with east-west. In this way, we can identify the direction of propagation of the waves (Figure 3a). The antennas are connected to a BNC connector and twisted bifilar and screen


**Figure 3a. The antennas and the receiver.**

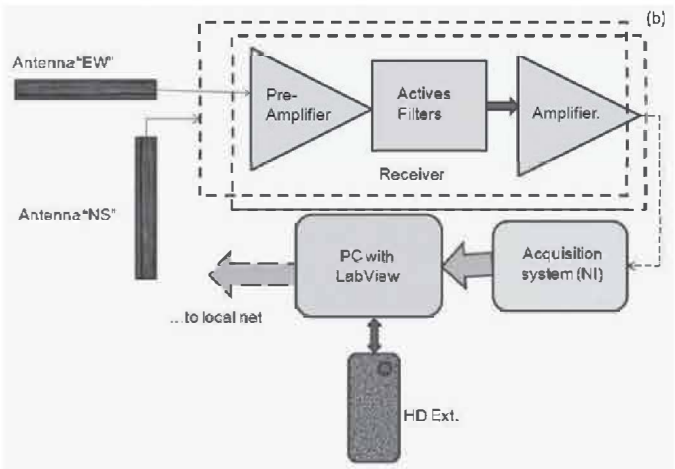


**Figure 3b. A block diagram of the station, with two identical channels.**

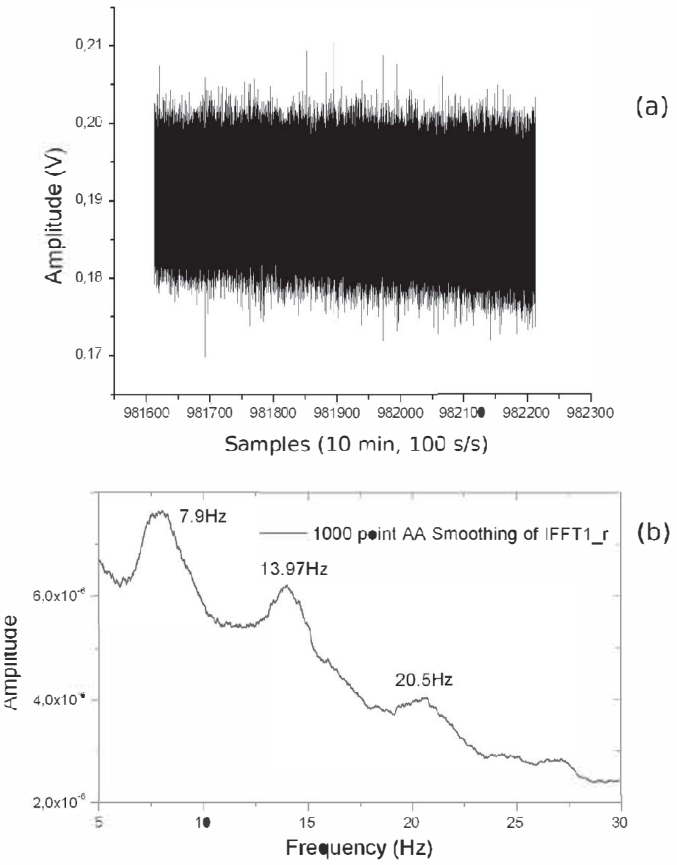


**Figure 4. An example of a register: (a) a 10-minute register; (b) the normalized amplitude spectrum, obtained with the FFT. The three harmonics are clearly observed. The time and date of the observation was 04:09 LT/19/04/12.**

to a physical ground at the receiver's connectors, each to an independent channel. Figure 3b shows the block diagram of the station.

We furthermore designed a board using the commercial software *PROTEUS*. We next tested the circuit with a setup to assure the proper performance of the receiver (offset, filters, amplifier levels, energy consumption and frequency response). We found that for the 10 Hz frequency, the receiver's gain was 43 dBV, and it had a consumption of 20 mA per channel and per feeding line (+6 V and −6 V). The filters allow us to suppress, through variable-precision resistors, those unwanted frequencies that we have identified in the circuit. We also found a low dependence between the gain and the feeding.

Currently, we are developing software that will allow us to transfer, store, and process the data, in order to directly have the Schumann-resonance spectra.

## 4. Preliminary Results and Discussion

In spite of the interference still present in the measurements, we have obtained a large number of spectra during the

first few months of operation (384 in total). In those spectra, we identified at least the first three harmonics of the Schumann resonance, although in several spectra we also identified the fourth Schumann-resonance harmonics (Figures 4a and 4b). The results of Figures 5a-5c and Figures 6a-6c correspond to April 9-15 and April 18 of 2012, between 00:00 and 08:00 local time (LT). The average values of the central frequency were within the reported results: 7.74 Hz, 14.11 Hz, and 20.22 Hz (Figures 7a-7c), consistent with the values reported by several authors. At other hours of the day, the presence of strong interference close to the Schumann-resonance harmonics made it very difficult to identify the Schumann-resonance spectra. The daily average behavior of the spectral frequency and amplitude of the studied samples indicated good time coherence among the first three Schumann-resonance harmonics (see Table 1 and Figure 8).

Nevertheless, we are still testing the most adequate place to locate the antennas in order to minimize interference.

We would like to point out that although this station has an old design, the results are different from those of other stations, because several Schumann-resonance perturbations are due to local electric discharges. By comparing the Schumann-resonance parameters of many stations, more-robust conclusions on the global climate can be obtained. Furthermore, as already shown in Figures 2 and 3, we do have some technical developments.

We are also planning to construct two more identical stations, forming a triangle: Mexico-Cuba-Central America. In this way, in quasi-real time we will have the state of the Schumann resonances in the region, and in both the north-south and east-west coordinates. We do not yet know how we will integrate the stations. It is very important to remark that we already have another two sets of antennas that are identical to the Mexican set.

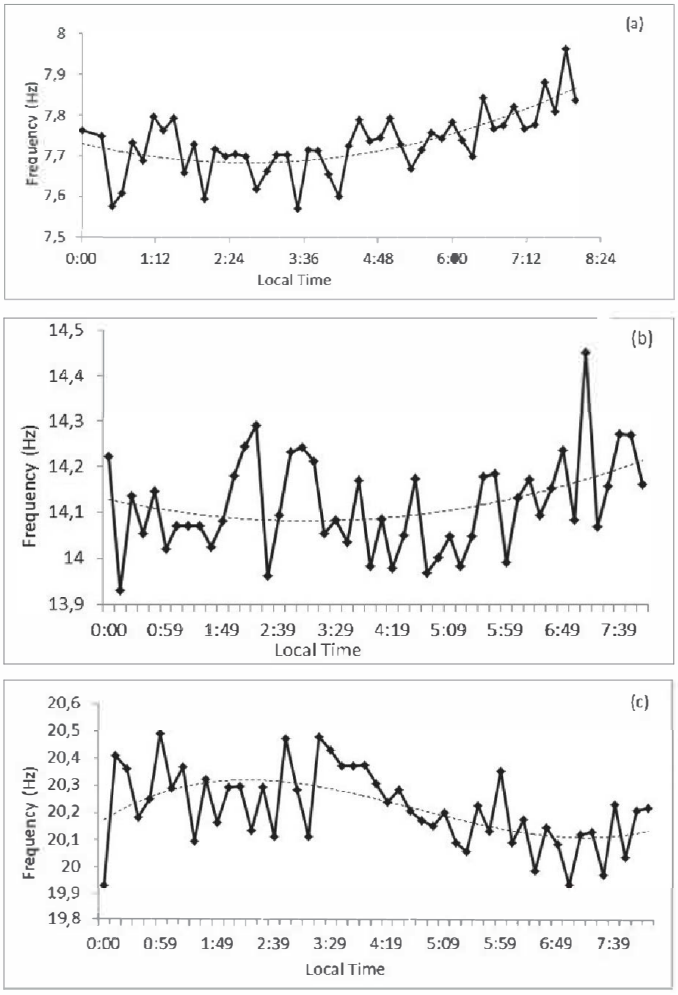


**Figure 5. An eight-day average frequency spectrum of the three first Schumann-resonance harmonics for the eight days analyzed: (a) first harmonic, (b) second harmonic, (c) third harmonic.**

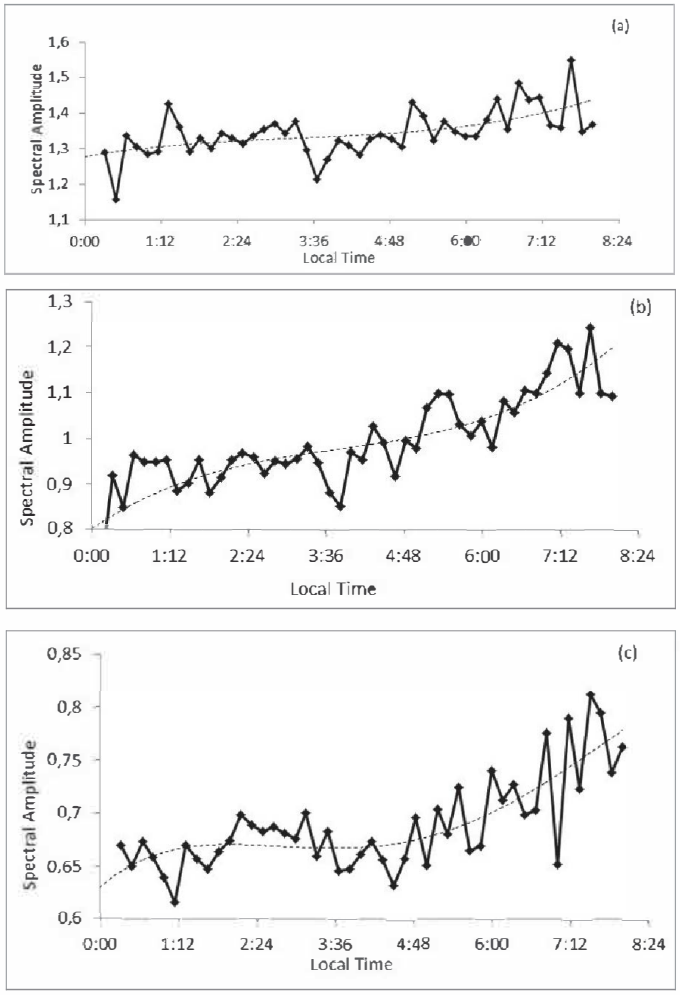


**Figure 6. The eight-day average spectral amplitude of the three first Schumann-resonance harmonics for the eight days analyzed: (a) first harmonic, (b) second harmonic, (c) third harmonic.**

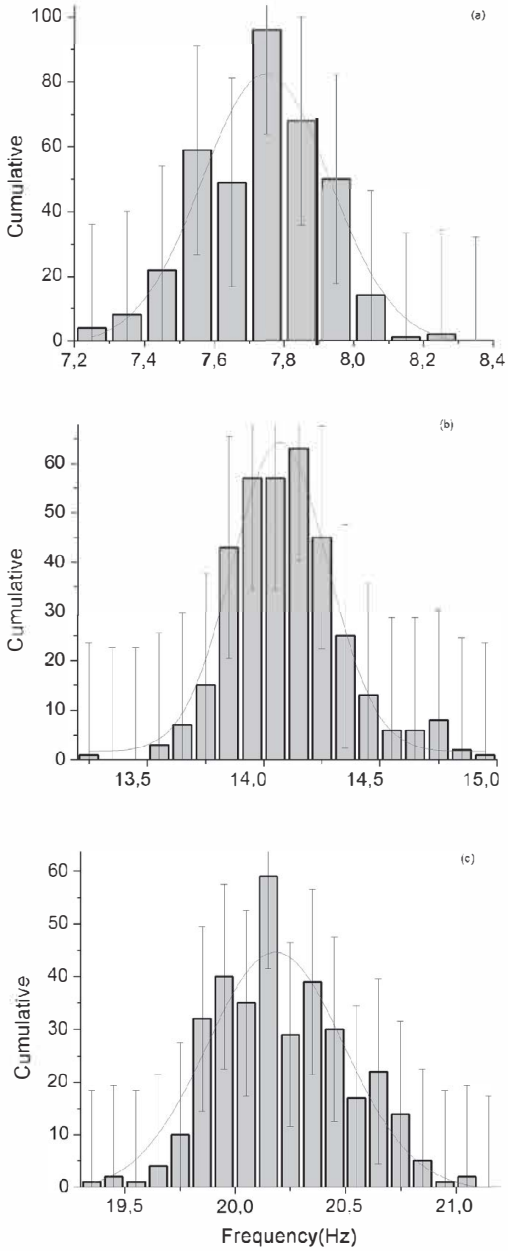


**Figure 7. The frequency counts for the first three Schumann-resonance harmonics of the analyzed sample (384 spectra). The dotted lines show the Gaussian adjusted to the distribution: (a) first harmonic, (b) second harmonic, (c) third harmonic.**

**Table 1. Frequency and spectral amplitude measurements of the first five harmonics of the Schumann resonances.**

| Day (April) | F1 | AF1 | F2 | AF2 | F3 | AF3 |
|---|---|---|---|---|---|---|
| 9 | 7.76 | 1.72 | 14.14 | 1.24 | 20.18 | 0.87 |
| 10 | 7.75 | 1.7 | 14.18 | 1.21 | 20.27 | 0.86 |
| 11 | 7.69 | 0.9 | 14.11 | 0.64 | 20.23 | 0.46 |
| 12 | 7.7 | 0.82 | 14.03 | 0.62 | 20.22 | 0.42 |
| 13 | 7.7 | 1.49 | 14.12 | 1.17 | 20.13 | 0.78 |
| 14 | 7.73 | 1.73 | 14.2 | 1.31 | 20.27 | 0.89 |
| 15 | 7.67 | 1.57 | 14.06 | 1.23 | 20.16 | 0.81 |
| 18 | 7.84 | 0.88 | 14.06 | 0.68 | 20.28 | 0.43 |
| **Average** | 7.73 | 1.35 | 14.11 | 1.01 | 20.22 | 0.69 |

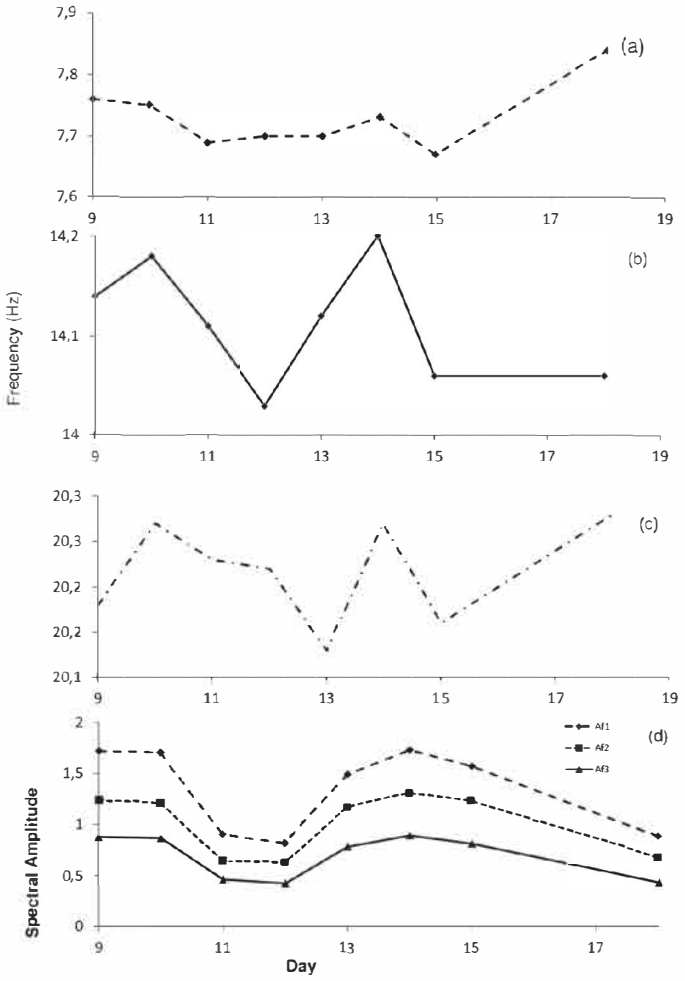


**Figure 8. The first three Schumann-resonance harmonics during the analyzed period: (a) the daily spectral amplitude averages; (b) the daily spectral frequency averages for the first harmonic; (c) the daily spectral frequency averages for the second harmonic; (d) the daily spectral frequency averages for the third harmonic. The dashed line corresponds to the first harmonic, the dotted line corresponds to the second harmonic, and the solid line corresponds to the third harmonic.**

## 5. Conclusions

We have presented preliminary results obtained from a Schumann-resonance station located in Mexico*** (19° 48' 19" N and longitude 101° 41' 39" W). The development of such a station is a tool for studies of geophysics, meteorology, the climate, the ionosphere, solar activity, and possibly human health. This station is the first of its kind in the region that includes Mexico, the Caribbean, and Central America. We measured Schumann-resonance harmonics at 7.74 Hz, 14.11 Hz, and 20.22 Hz, which are within the results reported by other authors. We need further calibration of the antennas in order to validate future reported data.

We believe that the results obtained so far allow us to state that the station is suitable for conducting systematic recordings that can carry out investigations in the region of interest.

## 6. Acknowledgements

This work was partially supported by grants DGAPA-UNAM IN103112-3 and CONACYT-Red de Ciencia y Tecnología Espacial (RedCyTE)-15.

## 7. References

1. W. O. Schumann. "Uberdestrahlundlosen eigenschwingungen einer leitenden kugel, die von einer luftschict und einer ionospharenhulle umgeben ist," *Naturforsch*, **7a**, 2, pp. 149-154, IDS: uw431, 1952, ISNN 0932-0784.

2. M. Balser and C. A. Wagner, "Observations of Earth-Ionosphere Cavity Resonances," *Nature*, **188**, 4751, November 1960, pp. 638-641.

3. G. Sátori, M. Neska, E. Williams, and K. Szendrő. "Signatures of the Day-Night Asymmetry of the Earth-Ionosphere Cavity in

High Time Resolution Schumann Resonance Records," *Radio Science*, **42**, 2, March 2007, RS2S10.

4. E. I. Yatsevich, A. P. Nickolaenko, and O. B. Pechonaya, "Diurnal and Seasonal Variations in the Intensities and Peak Frequencies of the First Three Schumann-Resonance Modes," *Radiophysics and Quantum Electronics*, **51**, 7, July 2008, pp. 528-538.

5. G. Sátori, "Monitoring Schumann Resonances-II. Daily and Seasonal Frequency Variations," *Journal of Atmospheric and Terrestrial Physics*, **58**, 13, September 1996, pp. 1483-1488.

6. D. Karakelian, S. L. Klemperer, A. S. Fraser-Smith, and G. C. Beroza, "A Transportable System for Monitoring Ultra Low Frequency Electromagnetic Signals Associated with Earthquakes," *Seismology Research Letters*, **71**, 4, July/ August 2000, pp. 423-436.

7. M. Hayakawa, M. K. Ohta, A. P. Nickolaenko, and Y. Ando, "Anomalous Effect in Schumann Resonance Phenomena Observed in Japan, Possibly Associated with the Chi-Chi Earthquake in Taiwan," *Annales Geophysicae*, **23**, 4, June 2005, pp. 1335-1346.

8. E. R. Williams, "The Schumann Resonance: A Global Tropical Thermometer," *Science*, **256**, 5060, May 1992, pp. 1184-1187.

9. A. P. Nickolaenko, G. Sátori, B. Zieger, L. M. Rabinowicz, and I. G. Kudintseva, "Parameters of Global Thunderstorm Activity Deduced from the Long-Term Schumann Resonance Records," *Journal of Atmospheric and Solar-Terrestrial Physics*, **60**, 3, February 1998, pp. 387-399.

10. R. Barr, D. L. Jones, and C. J. Rodger, "ELF and VLF Radio Waves," *Journal of Atmospheric and Solar-Terrestrial Physics*, **62**, 17-18. November-December 2000, pp. 1689-1718.

11. M. Sekiguchi, M. Hayakawa, A. P. Nickolaenko, and Y. Hobar, "Evidence on a Link Between the Intensity of Schumann Resonance and Global Surface Temperature," *Annales Geophysicae*, **24**, 7, August 2006, pp. 1809-1817.

12. V. C. Roldugin, Y. P. Maltsev, G. A. Petrova, and A. N. Vasiljev, "Decrease in the First Schumann Resonance Frequency During Solar Proton Events," *Journal of Geophysical Research*, **106**, A9, September 2001, pp. 18555-18562.

13. S. S. De, B. K. De, B. Bandyopadhyay, S. Paul, D. K. Haldar, and S. Baru, "Studies on the Shift in the Frequency of the First Schumann Resonance Mode During a Solar Proton Event, "*Journal of Atmospheric and Solar-Terrestrial Physics*," **72**, 11-12, July 2010, pp. 829-836.

14. A. Ondrášková, S. Ševčík, and P. Kostecký, "Decrease of Schumann Resonance Frequencies and Changes in the Effective Lightning Areas Toward the Solar Cycle Minimum of 2008-2009, "*Journal of Atmospheric and Solar-Terrestrial Physics*, **73**, 4, March 2011, pp. 534-543.

15. G. Mitsutake, K. Otsuka, M. Hayakawa, M. Sekiguchi, G. Cornélissen, and F. Halberg, "Does Schumann Resonance Affect Our Blood Pressure?," *Biomedicine & Pharmacotherapy*, **59**, Supplement 1, October 2005, pp. S10-S14.

16. S. J. Palmer, M. J. Rycroft, and M. Cermack, "Solar and Geomagnetic Activity, Extremely Low Frequency Magnetic and Electric Fields and Human Health at the Earth's Surface," *Surveys in Geophysics*, **27**, 5, September 2006, pp. 557-595.

17. W. F. Brian and R. C. Hannan, "Investigations of Relatively Easy to Construct Antennas with Efficiency in Receiving Schumann Resonances. Preparations for a Miniaturized Reconfigurable ELF Receiver," Langley Research Center, Hampton, Virginia, 2003, NASA/TM-2003-212647.

18. H. Michlmayr, "Magnetic Antennae for ULF. Detection and Recording of Schumann Resonances and Other Electromagnetic Phenomena at Frequencies Below 50 Hz," 2010, http://www.dxzone.com.